



Kent Academic Repository

Tsaousis, Anastasios D, Hamblin, Karleigh A., Elliot, Catherine, Gourlay, Campbell W., Moore, Anthony L. and van der Geizen, Mark (2018) *The human gut colonizer Blastocystis respire using Complex II and alternative oxidase to buffer transient oxygen fluctuations in the gut*. *Frontiers in Cellular and Infection Microbiology* . ISSN 2235-2988.

Downloaded from

<https://kar.kent.ac.uk/64950/> The University of Kent's Academic Repository KAR

The version of record is available from

<https://doi.org/10.3389/fcimb.2018.00371>

This document version

Author's Accepted Manuscript

DOI for this version

Licence for this version

CC BY (Attribution)

Additional information

Versions of research works

Versions of Record

If this version is the version of record, it is the same as the published version available on the publisher's web site. Cite as the published version.

Author Accepted Manuscripts

If this document is identified as the Author Accepted Manuscript it is the version after peer review but before type setting, copy editing or publisher branding. Cite as Surname, Initial. (Year) 'Title of article'. To be published in **Title of Journal** , Volume and issue numbers [peer-reviewed accepted version]. Available at: DOI or URL (Accessed: date).

Enquiries

If you have questions about this document contact ResearchSupport@kent.ac.uk. Please include the URL of the record in KAR. If you believe that your, or a third party's rights have been compromised through this document please see our [Take Down policy](https://www.kent.ac.uk/guides/kar-the-kent-academic-repository#policies) (available from <https://www.kent.ac.uk/guides/kar-the-kent-academic-repository#policies>).

The human gut colonizer *Blastocystis* respire using Complex II and alternative oxidase to buffer transient oxygen fluctuations in the gut

Anastasios D. Tsaousis¹, Karleigh A. Hamblin², Catherine R. Elliot³, Luke Young³, Alicia Rosell Hidalgo³, Campbell Gourlay¹, Anthony L. Moore³, Mark van der Giezen^{4*}

¹University of Kent, United Kingdom, ²Defence Science and Technology Laboratory, United Kingdom, ³University of Sussex, United Kingdom, ⁴University of Exeter, United Kingdom

Submitted to Journal:
Frontiers in Cellular and Infection Microbiology

Specialty Section:
Parasite and Host

Article type:
Original Research Article

Manuscript ID:
408353

Received on:
15 Jun 2018

Revised on:
24 Sep 2018

Frontiers website link:
www.frontiersin.org

Conflict of interest statement

The authors declare that the research was conducted in the absence of any commercial or financial relationships that could be construed as a potential conflict of interest

Author contribution statement

ADT, CWG, LY, ALM and MvdG designed the study. ADT, KAH, CRE, LY, ARH and CWG performed experiments. All authors analyzed the data. MvdG and ALM wrote the first draft and all authors reviewed and edited the final text.

Keywords

Alternative oxidase (AOX), Blastocystis, Oxygen, complex II, intestine, Salicylhydroxamic acid (SHAM), Octyl gallate, thenoyltrifluoroacetone (TTFA)

Abstract

Word count: 194

Blastocystis is the most common eukaryotic microbe in the human gut. It is linked to irritable bowel syndrome (IBS), but its role in disease has been contested considering its widespread nature. This organism is well adapted to its anoxic niche and lacks typical eukaryotic features such as a cytochrome-driven mitochondrial electron transport. Although generally considered a strict or obligate anaerobe, its genome encodes an alternative oxidase. Alternative oxidases are energetically wasteful enzymes as they are non-protonmotive and energy is liberated in heat, but they are considered to be involved in oxidative stress protective mechanisms. Our results demonstrate that the Blastocystis cells themselves respire oxygen via this alternative oxidase thereby casting doubt on its strict anaerobic nature. Inhibition experiments using alternative oxidase and Complex II specific inhibitors clearly demonstrate their role in cellular respiration. We postulate that the alternative oxidase in Blastocystis is used to buffer transient oxygen fluctuations in the gut and that it likely is a common colonizer of the human gut and not causally involved in IBS. Additionally the alternative oxidase could act as a protective mechanism in a dysbiotic gut and thereby explain the absence of Blastocystis in established IBS environments.

Funding statement

ADT was supported by BBSRC research grant (BB/M009971/1). KAH was supported by a Queen Mary PhD-studentship. Research in ALM's laboratory was supported by BBSRC BB/N010051/1. ARH gratefully acknowledges the receipt of a PhD studentship from the School of Life Sciences, University of Sussex. MvdG is grateful for support from the University of Exeter, Queen Mary University of London and the Wellcome Trust (078566/A/05/Z). The funders had no role in study design, data collection and analysis, decision to publish, or preparation of the manuscript.

Ethics statements

(Authors are required to state the ethical considerations of their study in the manuscript, including for cases where the study was exempt from ethical approval procedures)

Does the study presented in the manuscript involve human or animal subjects: No

1 **The human gut colonizer *Blastocystis* respire using Complex II and alternative oxidase**
2 **to buffer transient oxygen fluctuations in the gut**

3

4 Running title: *Blastocystis* uses an alternative oxidase to buffer oxygen fluctuations

5

6 Anastasios D. Tsaousis¹, Karleigh A. Hamblin^{2,3,*}, Catherine Elliot⁴, Luke Young⁴, Alicia
7 Rosell Hidalgo⁴, Campbell W. Gourlay⁵, Anthony L. Moore⁴ and Mark van der Giezen^{3,\$}

8

9

10 ¹Laboratory of Molecular & Evolutionary Parasitology, RAPID Group, School of
11 Biosciences, University of Kent, Canterbury CT2 7NJ, UK.

12 ²School of Biological and Chemical Sciences, Queen Mary University of London, Mile End,
13 London E1 4NS, UK.

14 ³Biosciences, University of Exeter, Stocker Road, Exeter EX4 4QD, UK.

15 ⁴Biochemistry and Biomedicine, School of Life Sciences, University of Sussex, Falmer,
16 Brighton BN1 9QG, UK.

17 ⁵Kent Fungal Group, School of Biosciences, University of Kent, Canterbury CT2 7NJ, UK.

18

19 ^{\$}Corresponding author:

20 Dr. Mark van der Giezen

21 email: m.vandergiezen@exeter.ac.uk

22 tel.: +44 1392 723 483

23 Twitter: MitoRem

24

25 ^{*}Current address:

26 CBR Division, Defence Science and Technology Laboratory, Porton Down, Salisbury, UK

27

28 Key words: *Blastocystis*, complex II, Alternative oxidase, gut microbiome, oxygen tolerance,
29 mitochondria

30

31

32 .

33 Abstract

34 *Blastocystis* is the most common eukaryotic microbe in the human gut. It is linked to irritable
35 bowel syndrome (IBS), but its role in disease has been contested considering its widespread
36 nature. This organism is well adapted to its anoxic niche and lacks typical eukaryotic features
37 such as a cytochrome-driven mitochondrial electron transport. Although generally considered
38 a strict or obligate anaerobe, its genome encodes an alternative oxidase. Alternative oxidases
39 are energetically wasteful enzymes as they are non-protonmotive and energy is liberated in
40 heat, but they are considered to be involved in oxidative stress protective mechanisms. Our
41 results demonstrate that the *Blastocystis* cells themselves respire oxygen via this alternative
42 oxidase thereby casting doubt on its strict anaerobic nature. Inhibition experiments using
43 alternative oxidase and Complex II specific inhibitors clearly demonstrate their role in cellular
44 respiration. We postulate that the alternative oxidase in *Blastocystis* is used to buffer transient
45 oxygen fluctuations in the gut and that it likely is a common colonizer of the human gut and
46 not causally involved in IBS. Additionally the alternative oxidase could act as a protective
47 mechanism in a dysbiotic gut and thereby explain the absence of *Blastocystis* in established
48 IBS environments.

49

50 Introduction

51 A healthy human gut is characterised by the presence of obligate anaerobic bacteria from the
52 Firmicutes and Bacteroides phyla who are considered to play a protective role in maintaining
53 the gut ecosystem (Donaldson et al., 2016). The establishment of this protective microbial
54 ecosystem in the gut has its origin within the first few days/weeks after birth and even the mode
55 of birth (caesarean or natural) can result in effects in later life (Sommer et al., 2017). The
56 resilience of the gut ecosystem, which co-evolved with humans, is illustrated by the fact that
57 generally, the gut flora returns to its original state after perturbations such as antibiotic
58 treatment or infections (Donaldson et al., 2016; Sommer et al., 2017). However, certain
59 perturbations can result in a detrimental new equilibrium that is not beneficial to the human
60 host. For example, an increase in facultative anaerobic *Enterobacteriaceae* is generally linked
61 to a dysbiosis of the gut, where an increase in the luminal bioavailability of oxygen causes a
62 shift in intestinal biodiversity (Byndloss et al., 2017; Rigottier-Gois, 2013; Rivera-Chávez et
63 al., 2017). Recently, a mechanistic coupling between gut microbes and the presence of
64 molecular oxygen was described by Byndloss *et al.* Activation of a colonocyte peroxisome
65 proliferator-activated receptor- γ (PPAR γ) results in reduction of the nitrate and oxygen
66 concentrations in the gut thereby controlling the proliferation of facultative anaerobes
67 (Byndloss et al., 2017). This clearly demonstrates a link between oxygen in the human intestine
68 and dysbiosis as previously hypothesised by Rigottier-Gois (2013).

69 Intestinal dysbiosis has been linked to several diseases including obesity and irritable bowel
70 diseases such as Crohn's disease and ulcerative colitis and to irritable bowel syndrome (IBS)
71 (Goulet, 2015; Rigottier-Gois, 2013). IBS is a common gastrointestinal disease presenting with
72 abdominal pain, constipation, diarrhoea and bloating (Enck et al., 2016). It is now generally
73 accepted that IBS is accompanied by a changed microbial gut flora (Simren et al., 2013) which
74 seems adapted to higher oxygen levels in the gut (Rigottier-Gois, 2013) based on reported
75 increases in *Enterobacteriaceae* in IBS patients (Carroll et al., 2012). Although most studies
76 focus on bacterial taxa in IBS patients, some studies have assessed the contribution of microbial
77 eukaryotes (Engsbro et al., 2012; Krogsgaard et al., 2015; Nash et al., 2017; Nourrisson et al.,
78 2014). Specifically, *Blastocystis* is frequently associated with IBS, however its role in disease
79 is contested (Ajajampur and Tan, 2016; Clark et al., 2013; Gentekaki et al., 2017; Stensvold and

80 van der Giezen, 2018). Although it is the most common microbial eukaryote of the human gut,
81 which can reach a prevalence of up to 100% (El Safadi et al., 2014), little is known about its
82 virulence (Ajjampur et al., 2016; Ajjampur and Tan, 2016). This limited amount of information
83 is compounded by the massive genetic diversity observed between isolates (Ajjampur and Tan,
84 2016; Gentekaki et al., 2017; Stensvold et al., 2007). Currently, *Blastocystis* is considered to
85 be a strict anaerobe (Zierdt, 1986), which makes its role in the IBS gut even more confusing,
86 especially considering the conflicting reports linking it to IBS (Krogsgaard et al., 2015;
87 Nourrisson et al., 2014). *Blastocystis* received additional attention due to its unusual
88 mitochondrion (Gentekaki et al., 2017; Lantsman et al., 2008; Müller et al., 2012; Stechmann
89 et al., 2008). As an anaerobe, and similar to other anaerobic microbial eukaryotes, it has lost
90 many classic features of mitochondria and performs no oxidative phosphorylation and lacks a
91 standard mitochondrial electron transport chain (see for example van der Giezen, 2011). It has
92 retained Complex I which supposedly maintains a proton motive force across the inner
93 membrane and passes electrons via rholoquinone to a fumarate reductase (Stechmann et al.,
94 2008) which acts as an alternative Complex II (Müller et al., 2012; Tielens et al., 2002). It has
95 also retained a mitochondrial genome (Pérez-Brocal and Clark, 2008). In addition to the
96 canonical mitochondrial iron-sulfur cluster assembly system *Blastocystis* also has a prokaryotic
97 SUF system that was localised in its cytosol (Tsaousis et al., 2012). Recently, it was also shown
98 that *Blastocystis* contains part of glycolysis in its mitochondrion (Bartulos et al., 2018).
99 Although *Blastocystis* can produce some ATP via substrate level phosphorylation using the
100 TCA cycle enzyme succinyl-CoA synthetase (Hamblin et al., 2008) it is mainly reliant on
101 fermentation producing lactate, acetate and probably propionate (Müller et al., 2012;
102 Stechmann et al., 2008). The *Blastocystis* mitochondrion is predicted to contain an alternative
103 oxidase which “should” accept electrons from Complex I and II (Standley and van der Giezen,
104 2012; Stechmann et al., 2008). Alternative oxidases are non-protonmotive quinol–oxygen
105 oxidoreductases which couple the oxidation of ubiquinol to the 4-electron reduction of
106 molecular oxygen to water (Moore and Albury, 2008). These enzymes are found in several
107 non-related organisms. Their physiological role is not completely clear but it has been
108 suggested to be involved in oxidative stress protective mechanisms, heat generation and to
109 maintain tricarboxylic acid cycle turnover under high cytosolic phosphorylation potential
110 (Moore and Albury, 2008). Alternative oxidases have been found in other parasites such as
111 *Cryptosporidium* (Roberts et al., 2004) and trypanosomes (Nihei et al., 2002). The trypanosome
112 homolog is well-studied as it is considered a potential drug target due to its absence in humans
113 (Shiba et al., 2013).

114 Here, we report the biochemical characterisation of an alternative oxidase in *Blastocystis* and
115 relate this to the organism’s ability to cope with fluctuating oxygen concentrations in the gut
116 and its postulated role in disease.

117

118 **Materials and methods**

119 *Organisms and culture conditions*

120 *Blastocystis* strain NandII cDNA was obtained from the *Blastocystis hominis* EST project
121 (Stechmann et al., 2008). Human *Blastocystis* sp. isolate DMP/02-328 was obtained during
122 routine screening and was grown at 36 °C with a mixed bacterial flora in LYSGM with 5%
123 adult bovine serum. Cells were grown under anoxic conditions and all culturing work
124 performed in an anaerobic chamber (Ruskinn SCI-tive with HEPA Hypoxia station). LYSGM
125 is a modification of TYSGM-9 in which the trypticase and yeast extract of the latter are
126 replaced with 0.25% yeast extract (Sigma) and 0.05% neutralized liver digest (Oxoid).

127 Subtyping of *Blastocystis* sp. DMP/02–328 indicated that this strain is subtype 4 (Stensvold et
128 al., 2007) whereas *Blastocystis* sp. NandII is subtype 1.

129 *Escherichia coli* strain α select silver efficiency (Bioline) was used for cloning and heme
130 deficient *E. coli* strain FN102 (Δ hemA (Km^R)) (Nihei et al., 2003) was used for recombinant
131 *Blastocystis* AOX expression.

132

133 *AOX cloning, expression and purification*

134 The putative AOX gene was originally identified in the *Blastocystis hominis* EST project
135 (<http://amoebidia.bcm.umontreal.ca/pepdb>) using BLASTn with the ESTs as queries. Full-
136 length genes were obtained by 5' and 3' rapid amplification of cDNA ends using the GeneRacer
137 Kit (Invitrogen). AOX sequences from *Blastocystis*, *Sauromatum guttatum* and *Trypanosoma*
138 *brucei* were aligned using ClustalW (Chenna et al., 2003) and examined.

139 *Blastocystis* AOX was amplified from cDNA using the forward primer 5'-aga aga *CAT ATG*
140 *TTC CCT ATC CTC TCC AGA GTC TTC* -3' and the reverse primer 5'-tct tct *GGA TCC TTA*
141 *CGC TTT CGT TGC GCC GTA CTT CG*-3' which added *NotI* and *BamHI* restriction sites
142 (indicated in italics) respectively. Amplification was carried out with Phusion High-Fidelity
143 DNA polymerase (New England Biolabs) yielding amplicons of the expected size
144 (approximately 0.9 kb). PCR products were purified using QIAquick Gel Extraction Kit
145 (QIAGEN), digested with *BamHI* and *NotI* restriction digestion enzymes and cloned into pET-
146 14b (Novagen). The pET-14b vector added a 6XHis tag to the N-terminus of AOX. The AOX
147 pET-14b plasmid was purified using QIAprep Spin Miniprep Kit (QIAGEN), sequenced to
148 confirm its validity (MWG) and used to transform FN102 *E. coli* cells.

149 FN102 membrane purification was carried out as described by Nihei et al. (2003) with minor
150 modifications. Briefly, starter cultures of K broth with ampicillin, kanamycin and
151 aminolevulinic acid (ALA) were inoculated and incubated at 37 °C until they reached an OD₆₀₀
152 of 0.1. Starter cultures were added to large scale cultures of K broth with carbenicillin until
153 they reached an OD₆₀₀ of 0.01. Large-scale cultures were grown at 30 °C until they reached
154 OD₆₀₀ of 0.1, induced with 100 μ M IPTG and incubated for 8 hours at 30 °C. Cells were
155 harvested by centrifugation at 3,500 g for 20 minutes at 4 °C. Harvested cells were resuspended
156 in 30 ml of Buffer S (60 mM Tris-HCl pH 7.5, 5 mM DTT, 300 mM NaCl, 20 % sucrose).
157 Cells were broken with a sonicator and centrifuged twice at 4,000 g for 10 minutes at 4 °C to
158 pellet cell debris. The supernatant was layered on top of buffer G (60 mM Tris-HCl pH 7.5, 5
159 mM DTT, 300 mM NaCl, 40 % sucrose) to create a sucrose gradient and centrifuged at 200,000
160 g for 1 hour at 4 °C. Pelleted membranes were resuspended in approximately 0.5 ml of buffer
161 S.

162

163 *AOX assay*

164 AOX activity was determined polarographically following uptake of oxygen using a Clark-
165 type electrode (Rank Brothers, Cambridge, U.K.) using 0.1–0.5 mg *E. coli* membranes
166 suspended in 0.4 ml air-saturated reaction medium (250 μ M at 25 °C) containing 50 mM Tris-
167 HCl (pH 7.5). Data were recorded digitally using a PowerLab/4SP system (ADInstruments Pty,
168 UK) with Chart version 3.6s software (ADInstruments).

169

170 *Western blotting*

171 *Blastocystis* whole-cell protein lysate, from strain DMP/02-328, was separated on a 10%
172 sodium dodecyl sulfate (SDS) polyacrylamide gel and blotted on to nitrocellulose membrane
173 (Bio-Rad). Anti-*Sauromatum guttatum* AOX (1:1,000) was used as primary antibody followed
174 by anti-mouse HRP conjugate (Pierce) 1:10,000 as a secondary antibody. Signal was detected
175 using a CN/DAB Substrate Kit (Pierce). Different cell fractions were isolated following
176 procedures previously described (Tsaousis et al., 2014). *Blastocystis* cells from NandII strain
177 (well-grown in media for 5 days) were harvested by centrifugation at $1,200 \times g$ for 10 min at 4
178 °C. Cells were resuspended in Locke's solution (pH 7.4) and pelleted again at the same speed
179 for the same duration. Cells were then broken with 40 strokes in a 10-ml Potter-Elvehjem tissue
180 homogenizer at 4 °C in isotonic buffer (200 mM sucrose, pH 7.2, 30 mM phosphate, 15 mM
181 β -mercaptoethanol, 30 mM NaCl, 0.6 mM CaCl₂, 0.6 mM KCl). Broken cells were diluted with
182 isotonic buffer and then centrifuged at $700 \times g$ for 10 min using a Sorvall RC-2B centrifuge to
183 remove unbroken cells. The supernatant was collected and centrifuged at $5,000 \times g$ for 20 min
184 to pellet the large granular fraction (LGF), where MROs are found (see Bartulos et al., 2018;
185 Lantsman et al., 2008; Tsaousis et al., 2014). The LGF was resuspended (washed) in isotonic
186 buffer and pelleted as described above. Finally, all fractions were stored at -20 °C in NuPAGE
187 LDS sample buffer along with 10 \times sample reducing agent (Invitrogen). Depending on the
188 amount of protein, 5 to 20 μ l of the supernatant was analyzed using a polyacrylamide mini gel
189 and subsequently blotted as above. Cellular fractions were analysed using anti-*Blastocystis*
190 hydrogenase (Stechmann et al., 2008) (1:250) and anti-*Blastocystis* SufCB (Tsaousis et al.,
191 2012) (1:500) antisera, as controls for the mitochondrial organelle and cytoplasm, respectively.
192 A loading control is shown in Figure 3B.

193

194 *Immunolocalization of AOX*

195 *Blastocystis* cells were resuspended in 1 X phosphate buffered saline (PBS) pH 7.4 and were
196 transferred to pretreated poly-L-lysine slides (Sigma). Slides were incubated at 4 °C for 2 hours
197 and then washed for 5 minutes in 1X PBS. The cells on the slides were fixed with 3.7%
198 formaldehyde/0.5% acetic acid for 15 minutes at 37 °C. Slides were washed for 5 minutes in
199 PBS/0.5% Tween-20 and then permeabilized with 0.1% Triton X-100 for 5 min. Washes were
200 performed three times for 5 minutes in PBS/0.05% Triton X-100 for 5 min. Fixed cells were
201 incubated for 30 minutes with a blocking solution of 5% skimmed milk powder in 1X PBS
202 solution (w/v) and then rinsed with 0.5% milk/PBS solution for 30 minutes. The cells were
203 then incubated with an anti-*S. guttatum* AOX antibody (1:100 dilution) in 1% milk/PBS
204 solution overnight at 4 °C. After three rinses in 1% milk/PBS for 10 minutes, the slides were
205 incubated with a fluorescent dye-labeled (Alexa 488 green) goat secondary antibody at a
206 dilution of 1:200. For colocalization experiments, before fixation, cells were incubated for 20
207 minutes with 200 nm of MitoTracker Red CMXRos (Molecular Probes). Cover slips were
208 mounted with anti-fade mounting medium (Vectashield) and observed under an Olympus IX81
209 fluorescence microscope. Images were collected using Micromanager 1.4 software and
210 processed with ImageJ.

211

212 *High-resolution respirometry*

213 Oxygen consumption was measured in *E. coli* control or AOX expressing cells using a high-
214 resolution respirometer (Oxygraph-2k; Oroboros) calibrated to 37 °C in LB media and data
215 recorded using DatLab software. Changes in the rate of oxygen consumption were measured
216 following repeated additions of salicylhydroxamic acid (SHAM) to give a final concentrations

217 of 1.2, 3.6, 7.0 and 9.4 mM or the appropriate volume of the carrier solvent (ethanol) as a
218 control.

219 Cultured *Blastocystis* cells were collected anaerobically and gently pelleted at $800 \times g$ for 10
220 minutes and re-suspended in sterile anoxic Locke's solution to a cell density of 1×10^6 cells/ml.
221 The oxygen consumption rate was measured using a high-resolution respirometer (Oxygraph-
222 2k; Oroboros) calibrated to 28 °C and data were recorded at 1 s intervals using DatLab
223 software. The effects on oxygen consumption following addition of the AOX inhibitor, SHAM
224 (Sigma), at 2.4 or 4.8 mM, or the succinate dehydrogenase inhibitor, TTFA (Sigma), at 5.4 or
225 11 μM as indicated. Ethanol was used as the solvent for both SHAM and TTFA whilst DMSO
226 was used for antimycin A (1 μM) (Sigma) and octylgallate (OG) (11 μM) (Sigma).

227

228 *Protein modelling*

229 *Blastocystis* AOX was modelled to the TAO crystal structure (PDB:5GN2) using the Swiss-
230 model software (<http://swissmodel.expasy.org/>) (Arnold et al., 2006; Benkert et al., 2011;
231 Biasini et al., 2014). The protein structure of *Blastocystis* AOX was loaded into MOE software
232 (Molecular Operating Environment, version 2016.08, Chemical Computing Group Inc.,
233 Montreal, Canada) for some preparatory steps to correct any structural issues. Hence, the
234 QuickPrep panel was used to optimise the hydrogen bond network using the Protonate 3D
235 algorithm and to perform an energy minimization on the system. AMBER99 forcefield was
236 used in assigning correct electronic charges and protonation of amino acid residues. The 3D
237 structure for rhodoquinol was built within MOE and energy minimized using the
238 Amber10:EHT forcefield. A second minimization was applied using the MOPAC semi-
239 empirical energy functions (PM3 Hamiltonian). Rhodoquinol was docked into the binding site
240 of the AOX using the Triangle Matcher placement method with London dG scoring.
241 Subsequently, poses resulting from the placement stage were further refined using the Induced
242 Fit method, which allows protein flexibility upon ligand binding, improving the prediction
243 accuracy for the interaction. Poses were then rescored using the GBVI/WSA dG scoring
244 function and the top five best scoring poses were retained.

245

246

247 **Results**

248 *AOX primary sequence analysis*

249 The AOX EST cluster originally identified in the *Blastocystis* NandII strain EST data
250 (Stechmann et al., 2008) appeared to be chimeric with a 40S ribosomal protein. Rapid
251 amplification of cDNA ends (RACE) allowed the full 5' and 3' ends of the AOX gene to be
252 obtained. The obtained sequence is identical to the one found in the recently completed
253 *Blastocystis* sp. NandII genome (Gentekaki et al., 2017). The *Blastocystis* AOX gene encodes
254 for a 304 amino acid protein with a predicted molecular weight of 35 kDa. The *Blastocystis*
255 AOX sequence has been deposited into GenBank (accession number: FJ647192).

256 *Blastocystis* NandII, *Sauromatum guttatum* and *Trypanosoma brucei* AOX sequences were
257 aligned to determine if residues known to be important for catalysis in other species were
258 present in the *Blastocystis* homologue. The alignment shown in Figure 1 clearly demonstrates
259 that many of the conserved features associated with AOX are present in the *Blastocystis*
260 sequence. A surface model of the *Blastocystis* AOX, using the trypanosomal alternative

261 oxidase (TAO) crystal structure as a template, is depicted in Figure 2A. The orange colouring
262 indicates the hydrophobic surface and the membrane face depicted in Figure 2A is the surface
263 which interacts with the mitochondrial inner membrane. Figure 2A also shows the hydrophobic
264 cavity leading to the di-iron centre. The residues lining the active site, which coordinate the
265 diiron centre, (namely the 1^o ligation sphere; *T. brucei* numbering throughout: E123, E162,
266 E213, E266, H165 and H269) are all conserved (Shiba et al., 2013) (Figure 2B). In addition,
267 Figure 2B also illustrates that residues involved in the 2^o ligation sphere (N161, Y220, D265,
268 Y246 & W247), which function in (Young et al., 2016b) electron transport and the oxygen
269 reduction cycle are also conserved in the *Blastocystis* sequence (Affourtit et al., 2002; Moore
270 and Albury, 2008).

271 Interestingly, however, several of the residues involved in substrate and inhibitor-binding are
272 different in *Blastocystis* compared to *T. brucei*. Although the majority of these residues are
273 conserved (such as R118, L122, E123, A216, E162, H165, L212, E213, A216 and E266),
274 several residues shown to interact with the tail of both substrate and inhibitors in *T. brucei* have
275 been modified (as depicted in Figure 2B: R96F, D100N and T219S). Since *Blastocystis* is an
276 anaerobe it seems unlikely that it utilises ubiquinone as substrate but probably uses rhodoquinol
277 instead (Stairs et al., 2018) which operates at a much lower midpoint potential.

278 In order to assess the influence of these substitutions upon substrate binding, docking studies
279 of rhodoquinol were undertaken using the homology model described in Figure 2C and D. As
280 shown in Figure 2C, rhodoquinol is bound in a fashion analogous to the position determined
281 for ubiquinol within the TAO crystal structure (Shiba et al., 2013), with the binding positions
282 for 1-OH and 4-OH positioned between the iron core and T219S respectively. What is apparent
283 from Figures 2C and D is that the proposed proton transfer network within TAO (involving
284 R96, D100 and E215) (Young et al., 2016a) is completely missing, and appears to have been
285 replaced instead by a single histidine. Given the proximity of this histidine to the proposed
286 rhodoquinol binding site, ~2.9 Å from the OH, and the likelihood it has free rotation around
287 the R-group due to lack of a secondary binding point, it is highly likely that the histidine is able
288 to act as a pathway for proton removal to solvent, thereby fulfilling a similar role within the
289 quinol reactivity mechanism as the previously described pathway (Young et al., 2016b).

290 As rhodoquinol is subtly different from ubiquinone, the residues which are different from *T.*
291 *brucei* TAO might actually coordinate the rhodoquinol in the *Blastocystis* AOX. In agreement
292 with this assertion is the discovery of *RquA* on the *Blastocystis* genome (Gentekaki et al., 2017;
293 Stairs et al., 2018), a gene thought to encode an enzyme of the rhodoquinone biosynthetic
294 pathway (Lonjers et al., 2012; Stairs et al., 2018). Similar to other parasites including
295 microsporidia, *Blastocystis* does not contain any of the cysteine residues which, in plants at
296 least, are thought to be involved in AOX activation by pyruvate (Rhoads et al., 1998). Its
297 absence in *Blastocystis* suggests that this organism, similar to the microsporidian and the
298 trypanosomal AOX, is not regulated by α -keto acids. In addition, T124 which has been linked
299 to changes in oxygen affinity (Moore and Albury, 2008) has been changed to a serine residue
300 in *Blastocystis*.

301

302 *Blastocystis* AOX protein is mitochondrial

303 Comparing the *Blastocystis* AOX sequence with the *Sauromatum guttatum* AOX indicates that
304 the epitope for the *S. guttatum* AOX monoclonal antibody (RADEAHHRDVNH) is quite
305 conserved in *Blastocystis* NandII. Of the twelve residues, ten are identical (see Figure 1). We
306 therefore decided to test the *S. guttatum* antibody on *Blastocystis* NandII total protein extracts.
307 Western blotting of *Blastocystis* fractions detected a single protein, which is enriched in the

308 mitochondrial fraction, of approximately 29 kDa, in reasonable agreement with the predicted
309 molecular weight for the *Blastocystis* AOX (Supplementary Figure 1A). Targeting signal
310 predictions such as Mitoprot (Claros and Vincens, 1996) and pSORT (Horton et al., 2007)
311 failed to predict a mitochondrial targeting signal which could have explained the size difference
312 between the observed and calculated molecular weight of the *Blastocystis* AOX. Amino acid
313 composition and globularity of a protein do play a role in the actual observed molecular weight
314 and membrane proteins are known to have issues in this regard (Rath et al., 2009). Using the
315 anti-AOX antibody on *Blastocystis* cellular fractions clearly indicated an enrichment in
316 mitochondria (Figure 3A). The AOX band appeared in the mitochondrial fraction, but absent
317 in the cytosolic fraction, consistent with the absence of this protein in *Blastocystis* MROs. The
318 anti-*Blastocystis* hydrogenase antisera shows specific detection of *Blastocystis* hydrogenase
319 (Stechmann et al., 2008) in the MRO fraction (MRO positive control) while the anti-
320 *Blastocystis* SufCB antiserum shows specific detection of *Blastocystis* SufCB (Tsaousis et al.,
321 2014) in the cytosolic fraction (positive control for cytosolic fraction).

322

323 The *S. guttatum* AOX monoclonal antibody was subsequently used to localize the AOX within
324 *Blastocystis* cells using immunofluorescence microscopy. The AOX antibody signal was found
325 to co-localize with MitoTracker Red CMXRos (Figure 4), a mitochondrion-specific stain
326 which has been used previously on *Blastocystis* mitochondria (Stechmann et al., 2008;
327 Stechmann et al., 2009; Tsaousis et al., 2012). It also co-localized with the mitochondrial DAPI
328 label in agreement with the presence of an organellar genome (Nasirudeen and Tan, 2004;
329 Pérez-Brocal and Clark, 2008). This clearly suggests that AOX localized to the mitochondrion-
330 related organelle found in *Blastocystis*.

331

332 *Blastocystis* AOX complements heme deficient *E. coli*

333 To assay AOX activity, the *Blastocystis* AOX gene was expressed in a heme deficient
334 *Escherichia coli* strain (FN102 (Δ hemA (Km^R)) (Nihei et al., 2003)), where the gene for
335 glutamyl-tRNA reductase, the first enzyme in heme biosynthesis, has been replaced with a
336 kanamycin resistance gene. Expressing AOX in this strain complements for the heme
337 deficiency as it provides *E. coli* with an additional terminal oxidase which does not require
338 heme for activity (Fukai et al., 2003). Therefore, heme deficient cells expressing recombinant
339 AOX do not require the addition of aminolevulinic acid, a heme precursor, which heme
340 deficient cells normally require for aerobic growth (Fukai et al., 2003). In addition, expressing
341 AOX in a heme deficient mutant reduces the potential for confusing AOX activity with the
342 activity of other quinol oxidases. The main oxidases in *E. coli* use heme prosthetic groups for
343 activity. *E. coli* FN102 cells capable of growth without aminolevulinic acid were further
344 analysed for the presence of the *Blastocystis* AOX. This protein could indeed be detected in a
345 purified membrane fraction from the heme deficient *E. coli* FN102 strain (Supplementary
346 Figures 1B and 2).

347

348 *Blastocystis* AOX uses oxygen and duroquinol and is sensitive to octyl gallate.

349 The activity of AOX can be measured by oxygen uptake with quinols as substrates. Figure 5A
350 shows the results of measuring oxygen uptake in the purified membranes of heme deficient *E.*
351 *coli* expressing recombinant *Blastocystis* AOX. Addition of duroquinol (Sigma), an AOX
352 substrate, initiates oxygen consumption indicating that oxygen uptake only occurs in the

353 presence of quinols. Oxygen consumption is almost completely abated by the addition of
354 octylgallate, an AOX inhibitor, clearly indicating that the oxygen consumption was due to the
355 activity of an AOX. To demonstrate that the *Blastocystis* AOX is also sensitive to
356 salicylhydroxamic acid (SHAM), another AOX inhibitor, we measured the oxygen
357 consumption rate of the heme deficient *E. coli* FN102 strain expressing the *Blastocystis* AOX
358 in whole cells. Similarly, oxygen consumption was affected by the AOX inhibitor (Figure 5B).
359 Together, this data suggests that the *Blastocystis* AOX consumes oxygen in the presence of
360 quinols and is sensitive to typical AOX inhibitors.

361

362 *Blastocystis* cells respire molecular oxygen

363 In order to assess whether *Blastocystis* cells themselves are able to use molecular oxygen *in*
364 *vivo*, whole *Blastocystis* cells were analysed in a high-resolution respirometer. The oxygen
365 consumption rate was measured in washed *Blastocystis* NandII cells at a density of 1×10^6
366 cells/ml at 28 °C. Live *Blastocystis* cells consumed oxygen and this activity was affected by
367 addition of SHAM (Figure 6A). As AOX receives its electrons from Complex II (succinate
368 dehydrogenase/fumarate reductase), we tested the effect of the Complex II inhibitor
369 thenoyltrifluoroacetone (TTFA) on *Blastocystis* oxygen consumption. Similar to SHAM,
370 exposure to TTFA also affects the oxygen consumption rate of *Blastocystis in vivo* (Figure 6B)
371 suggesting the *Blastocystis* AOX does indeed receive its reducing equivalents via Complex II
372 (see Supplementary Figure 3 for controls).

373

374 Discussion

375 *Blastocystis* is the most common eukaryotic inhabitant of the human gut (Gentekaki et al.,
376 2017). It has been marred by confusion almost from its first discovery in the 19th century when
377 it was linked to cholera (see Zierdt, 1991). It has since then been associated with almost every
378 eukaryotic domain until it was clearly shown to be a member of the large stramenopile lineage
379 (Silberman et al., 1996). Stramenopiles are an extremely diverse grouping and can be found in
380 many environments. It includes major plant pathogens such as *Phytophthora*, but also diatoms
381 which are major primary producers in the world's oceans. Together with *Pythium* (Hilton et
382 al., 2016), *Blastocystis* is thought to be the only human pathogen in this eukaryotic lineage.
383 However, reports about its supposed pathogenicity or role in disease are conflicting (see for
384 example Clark et al., 2013; Miller and Minshew, 1988; Stensvold and van der Giezen, 2018).
385 Presence of *Blastocystis* in stool samples of patients with gastrointestinal complaints has
386 repeatedly been reported. However, as it a faecally-orally transmitted organism, people with
387 *Blastocystis* in their intestines might also have been exposed to other potential pathogens and
388 a causative relationship between disease and *Blastocystis* has never been demonstrated.

389 In the literature, *Blastocystis* is often associated with irritable bowel syndrome (IBS) although
390 here again, the literature is conflicting. Several cohort studies suggest a link between
391 *Blastocystis* and IBS (Jimenez-Gonzalez et al., 2012; Nourrisson et al., 2014; Yakoob et al.,
392 2010) while others do not (Beghini et al., 2017; Krogsgaard et al., 2015; Petersen et al., 2013).
393 A possible explanation for these disparate findings is the large genetic diversity observed
394 within *Blastocystis* (Gentekaki et al., 2017) where some subtypes might indeed be linked to
395 disease while others might not (Stensvold et al., 2007).

396 A factor that has thus far been overlooked in this respect is the fact that *Blastocystis* is
397 considered to be a strict anaerobe (Zierdt, 1986) as it is incapable of oxidative phosphorylation

398 (Fenchel and Finlay, 1995). Genomic studies confirm the notion that *Blastocystis* is indeed
399 incapable of oxidative phosphorylation as the classic cytochrome *c* oxidase (Complex IV) is
400 absent from its genome (Denoeud et al., 2011; Gentekaki et al., 2017). Indeed, only Complex
401 I and II are present suggesting an anaerobic energy metabolism (Müller et al., 2012). The
402 presence of an alternative oxidase in *Blastocystis* is therefore somewhat surprising as it
403 suggests its energy metabolism might not be completely independent of molecular oxygen.
404 Alternative oxidases are generally considered to be energetically wasteful enzymes as they
405 normally short-circuit the mitochondrial electron transport chain by shuttling reducing
406 equivalents from Complex I or II away from the proton translocating respiratory pathway to
407 molecular oxygen without pumping protons across the mitochondrial inner membrane (May et
408 al., 2017; Shiba et al., 2013). In plants AOX acts as a redox sink under stress conditions such
409 as through respiratory inhibition or drought thereby reducing the formation of deleterious
410 reactive oxygen species (ROS) production.

411 It is interesting to speculate as to whether it plays a similar role in *Blastocystis* by not only
412 providing a route of electron transport from Complex I and II, and in doing so generate a
413 protonmotive force via Complex I, but also reduce ROS production at Complex I and through
414 reversed electron transport from Complex II. Obviously, further experiments are required to
415 substantiate such a notion. Nevertheless the result that the Complex II inhibitor
416 thenoyltrifluoroacetone inhibits alternative oxidase function in whole *Blastocystis* cells
417 suggests that the alternative oxidase operates indeed via Complex II as in other organisms
418 (Stechmann et al., 2008)

419 The oxygen concentration in a healthy gut is extremely low (Albenberg et al., 2014) to support
420 growth of obligate anaerobic bacteria from the Firmicutes and Bacteroides phyla. These
421 bacteria are important in maintaining a healthy gut ecosystem (Donaldson et al., 2016). When
422 the microbial flora in the gut gets disturbed as in a dysbiotic gut, facultative anaerobic
423 *Enterobacteriaceae* establish themselves resulting in an increase of the oxygen concentration
424 (Byndloss et al., 2017; Rigottier-Gois, 2013; Rivera-Chávez et al., 2017). This suggests that
425 for a strict anaerobe such as *Blastocystis*, a dysbiotic gut is not the most ideal ecosystem and
426 that similarly to obligate anaerobic bacteria, it no longer can maintain itself in this niche. Our
427 data suggests that its alternative oxidase might allow it to deal with fluctuating oxygen
428 concentrations that it might encounter in the gut. Similarly, it was previously shown that
429 *Blastocystis* also has other mechanisms to deal with such oxygen fluctuations. In addition to
430 the standard eukaryotic mitochondrial oxygen-sensitive iron-sulfur cluster assembly system,
431 *Blastocystis* contains a SufCB protein that is expressed under oxygen-stressed conditions
432 (Tsaousis et al., 2012). This might explain why some studies do not find *Blastocystis* in IBS
433 patients (Beghini et al., 2017; Krogsgaard et al., 2015; Petersen et al., 2013) and others do
434 (Jimenez-Gonzalez et al., 2012; Nourrisson et al., 2014; Yakoob et al., 2010). In well-
435 established IBS guts, the dysbiosis might have driven *Blastocystis* out of the gut while in early
436 stages of disease, the normal gut colonizer might attempt to stay by means of utilizing its
437 alternative oxidase to protect itself from molecular oxygen as has been suggested earlier
438 (Gomes et al., 2001; Stensvold and van der Giezen, 2018). Overall, our data suggests that
439 *Blastocystis* can cope with fluctuating oxygen concentrations that it might encounter in the
440 human gut and might be better described as a microaerophile. However, considering its overall
441 oxygen-independent energy metabolism (Gentekaki et al., 2017; Müller et al., 2012), it seems
442 unlikely that the dysbiotic gut of IBS patients is a suitable habitat for this anaerobe.

443

444 **Abbreviations**

445 AOX: Alternative Oxidase
446 DDT: Dichloro Diphenyl Trichloroethane
447 EST: Expressed Sequence Tag
448 IBS: Irritable Bowel Syndrome
449 ROS: Reactive Oxygen Species
450 SHAM: Salicylhydroxamic acid
451 TAO: Trypanosomal Alternative Oxidase
452 TTFA: Thenoyltrifluoroacetone

453

454

455 **Declarations:**

456 The authors have declared that the research was conducted in the absence of any commercial
457 or financial relationships that could be construed as a potential conflict of interest

458 Funding was provided by the BBSRC and Wellcome Trust.

459

460 **Acknowledgements**

461 ADT was supported by BBSRC research grant (BB/M009971/1). KAH was supported by a
462 Queen Mary PhD-studentship. Research in ALM's laboratory was supported by BBSRC
463 BB/N010051/1. ARH gratefully acknowledges the receipt of a PhD studentship from the
464 School of Life Sciences, University of Sussex. MvdG is grateful for support from the
465 University of Exeter, Queen Mary University of London and the Wellcome Trust
466 (078566/A/05/Z).

467

468 **References**

469 Affourtit, C., Albury, M.S., Crichton, P.G., and Moore, A.L. (2002). Exploring the molecular nature of
470 alternative oxidase regulation and catalysis. *FEBS Lett* 510, 121-126.
471 Ajjampur, S.S., Png, C.W., Chia, W.N., Zhang, Y., and Tan, K.S. (2016). *Ex vivo* and *in vivo* mice models
472 to study *Blastocystis* spp. adhesion, colonization and pathology: Closer to proving Koch's postulates.
473 *PLoS ONE* 11, e0160458.
474 Ajjampur, S.S., and Tan, K.S. (2016). Pathogenic mechanisms in *Blastocystis* spp. - Interpreting results
475 from *in vitro* and *in vivo* studies. *Parasitology international* 65, 772-779.
476 Albenberg, L., Esipova, T.V., Judge, C.P., Bittinger, K., Chen, J., Laughlin, A., Grunberg, S., Baldassano,
477 R.N., Lewis, J.D., Li, H., *et al.* (2014). Correlation between intraluminal oxygen gradient and radial
478 partitioning of intestinal microbiota. *Gastroenterology* 147, 1055-1063.e1058.
479 Arnold, K., Bordoli, L., Kopp, J., and Schwede, T. (2006). The SWISS-MODEL workspace: a web-based
480 environment for protein structure homology modelling. *Bioinformatics* 22, 195-201.
481 Bartulos, C.R., Rogers, M.B., Williams, T.A., Gentekaki, E., Brinkmann, H., Cerff, R., Liaud, M.F., Hehl,
482 A.B., Yarlett, N.R., Gruber, A., *et al.* (2018). Mitochondrial glycolysis in a major lineage of eukaryotes.
483 *Genome biology and evolution*.

484 Beghini, F., Pasolli, E., Truong, T.D., Putignani, L., Caccio, S.M., and Segata, N. (2017). Large-scale
485 comparative metagenomics of *Blastocystis*, a common member of the human gut microbiome. *ISME*
486 *J 11*, 2848-2863.

487 Benkert, P., Biasini, M., and Schwede, T. (2011). Toward the estimation of the absolute quality of
488 individual protein structure models. *Bioinformatics 27*, 343-350.

489 Biasini, M., Bienert, S., Waterhouse, A., Arnold, K., Studer, G., Schmidt, T., Kiefer, F., Cassarino, T.G.,
490 Bertoni, M., Bordoli, L., *et al.* (2014). SWISS-MODEL: modelling protein tertiary and quaternary
491 structure using evolutionary information. *Nucleic Acids Res 42*, W252-W258.

492 Byndloss, M.X., Olsan, E.E., Rivera-Chavez, F., Tiffany, C.R., Cevallos, S.A., Lokken, K.L., Torres, T.P.,
493 Byndloss, A.J., Faber, F., Gao, Y., *et al.* (2017). Microbiota-activated PPAR-gamma signaling inhibits
494 dysbiotic Enterobacteriaceae expansion. *Science 357*, 570-575.

495 Carroll, I.M., Ringel-Kulka, T., Siddle, J.P., and Ringel, Y. (2012). Alterations in composition and
496 diversity of the intestinal microbiota in patients with diarrhea-predominant irritable bowel
497 syndrome. *Neurogastroenterol Motil 24*, 521-530, e248.

498 Chenna, R., Sugawara, H., Koike, T., Lopez, R., Gibson, T.J., Higgins, D.G., and Thompson, J.D. (2003).
499 Multiple sequence alignment with the Clustal series of programs. *Nucleic Acids Res 31*, 3497-3500.

500 Clark, C.G., van der Giezen, M., Alfellani, M.A., and Stensvold, C.R. (2013). Recent developments in
501 *Blastocystis* research. *Adv Parasitol 82*, 1-32.

502 Claros, M.G., and Vincens, P. (1996). Computational method to predict mitochondrially imported
503 proteins and their targeting sequences. *Eur J Biochem 241*, 779-786.

504 Denoëud, F., Roussel, M., Noel, B., Wawrzyniak, I., Da Silva, C., Diogon, M., Viscogliosi, E., Brochier-
505 Armanet, C., Couloux, A., Poulain, J., *et al.* (2011). Genome sequence of the stramenopile
506 *Blastocystis*, a human anaerobic parasite. *Genome Biol 12*, R29.

507 Donaldson, G.P., Lee, S.M., and Mazmanian, S.K. (2016). Gut biogeography of the bacterial
508 microbiota. *Nat Rev Microbiol 14*, 20-32.

509 El Safadi, D., Gaayeb, L., Meloni, D., Cian, A., Poirier, P., Wawrzyniak, I., Delbac, F., Dabboussi, F.,
510 Delhaes, L., Seck, M., *et al.* (2014). Children of Senegal River Basin show the highest prevalence of
511 *Blastocystis* sp. ever observed worldwide. *BMC Infectious Diseases 14*, 164.

512 Enck, P., Aziz, Q., Barbara, G., Farmer, A.D., Fukudo, S., Mayer, E.A., Niesler, B., Quigley, E.M., Rajilic-
513 Stojanovic, M., Schemann, M., *et al.* (2016). Irritable bowel syndrome. *Nat Rev Dis Primers 2*, 16014.

514 Engsbro, A.L., Stensvold, C.R., Nielsen, H.V., and Bytzer, P. (2012). Treatment of *Dientamoeba fragilis*
515 in patients with irritable bowel syndrome. *Am J Trop Med Hyg 87*, 1046-1052.

516 Fenchel, T., and Finlay, B.J. (1995). *Ecology and evolution in anoxic worlds* (Oxford: Oxford University
517 Press).

518 Fukai, Y., Nihei, C., Kawai, K., Yabu, Y., Suzuki, T., Ohta, N., Minagawa, N., Nagai, K., and Kita, K.
519 (2003). Overproduction of highly active trypanosome alternative oxidase in *Escherichia coli* heme-
520 deficient mutant. *Parasitol Int 52*, 237-241.

521 Gentekaki, E., Curtis, B., Stairs, C., Klimes, V., Elias, M., Salas, D., Herman, E., Eme, L., Arias, M.C.,
522 Hilliou, F., *et al.* (2017). Extreme genome diversity in the hyper-prevalent parasitic eukaryote
523 *Blastocystis*. *PLoS Biol 15*, e2003769.

524 Gomes, C.M., Le Gall, J., Xavier, A.V., and Teixeira, M. (2001). Could a diiron-containing four-helix-
525 bundle protein have been a primitive oxygen reductase? *Chembiochem 2*, 583-587.

526 Goulet, O. (2015). Potential role of the intestinal microbiota in programming health and disease.
527 *Nutr Rev 73 Suppl 1*, 32-40.

528 Hamblin, K., Standley, D.M., Rogers, M.B., Stechmann, A., Roger, A.J., Maytum, R., and van der
529 Giezen, M. (2008). Localisation and nucleotide specificity of *Blastocystis* succinyl-CoA synthetase.
530 *Mol Microbiol 68*, 1395-1405.

531 Hilton, R.E., Tepedino, K., Glenn, C.J., and Merkel, K.L. (2016). Swamp cancer: a case of human
532 pythiosis and review of the literature. *British Journal of Dermatology 175*, 394-397.

533 Horton, P., Park, K.J., Obayashi, T., Fujita, N., Harada, H., Adams-Collier, C.J., and Nakai, K. (2007).
534 WoLF PSORT: protein localization predictor. *Nucleic Acids Res 35*, W585-587.

535 Jimenez-Gonzalez, D.E., Martinez-Flores, W.A., Reyes-Gordillo, J., Ramirez-Miranda, M.E., Arroyo-
536 Escalante, S., Romero-Valdovinos, M., Stark, D., Souza-Saldivar, V., Martinez-Hernandez, F., Flisser,
537 A., *et al.* (2012). *Blastocystis* infection is associated with irritable bowel syndrome in a Mexican
538 patient population. *Parasitol Res* 110, 1269-1275.

539 Krogsgaard, L.R., Engsbro, A.L., Stensvold, C.R., Nielsen, H.V., and Bytzer, P. (2015). The prevalence
540 of intestinal parasites is not greater among individuals with irritable bowel syndrome: a population-
541 based case-control study. *Clin Gastroenterol Hepatol* 13, 507-513 e502.

542 Lantsman, Y., Tan, K.S.W., Morada, M., and Yarlett, N. (2008). Biochemical characterization of a
543 mitochondrial-like organelle from *Blastocystis* sp. subtype 7. *Microbiol* 154, 2757-2766.

544 Lonjers, Z.T., Dickson, E.L., Chu, T.P., Kreutz, J.E., Neacsu, F.A., Anders, K.R., and Shepherd, J.N.
545 (2012). Identification of a new gene required for the biosynthesis of rodoquinone in *Rhodospirillum*
546 *rubrum*. *J Bacteriol* 194, 965-971.

547 May, B., Young, L., and Moore, A.L. (2017). Structural insights into the alternative oxidases: are all
548 oxidases made equal? *Biochem Soc Trans* 45, 731-740.

549 Miller, R.A., and Minshew, B.H. (1988). *Blastocystis hominis*: an organism in search of a disease. *Rev*
550 *Infect Dis* 10, 930-938.

551 Moore, A.L., and Albury, M.S. (2008). Further insights into the structure of the alternative oxidase:
552 from plants to parasites. *Biochem Soc Trans* 36, 1022-1026.

553 Müller, M., Mentel, M., van Hellemond, J.J., Henze, K., Wöhle, C., Gould, S.B., Yu, R.-Y., van der
554 Giezen, M., Tielens, A.G., and Martin, W.F. (2012). Biochemistry and evolution of anaerobic energy
555 metabolism in eukaryotes. *Microbiol Mol Biol Rev* 76, 444-495.

556 Nash, A.K., Auchtung, T.A., Wong, M.C., Smith, D.P., Gesell, J.R., Ross, M.C., Stewart, C.J., Metcalf,
557 G.A., Muzny, D.M., Gibbs, R.A., *et al.* (2017). The gut mycobiome of the Human Microbiome Project
558 healthy cohort. *Microbiome* 5, 153.

559 Nasirudeen, A.M., and Tan, K.S. (2004). Isolation and characterization of the mitochondrion-like
560 organelle from *Blastocystis hominis*. *J Microbiol Methods* 58, 101-109.

561 Nihei, C., Fukai, Y., Kawai, K., Osanai, A., Yabu, Y., Suzuki, T., Ohta, N., Minagawa, N., Nagai, K., and
562 Kita, K. (2003). Purification of active recombinant trypanosome alternative oxidase. *FEBS Lett* 538,
563 35-40.

564 Nihei, C., Fukai, Y., and Kita, K. (2002). Trypanosome alternative oxidase as a target of
565 chemotherapy. *Biochimica et Biophysica Acta (BBA) - Molecular Basis of Disease* 1587, 234-239.

566 Nourrisson, C., Scanzi, J., Pereira, B., NkoudMongo, C., Wawrzyniak, I., Cian, A., Viscogliosi, E., Livrelli,
567 V., Delbac, F., Dapoigny, M., *et al.* (2014). *Blastocystis* is associated with decrease of fecal microbiota
568 protective bacteria: comparative analysis between patients with irritable bowel syndrome and
569 control subjects. *PLoS ONE* 9, e111868.

570 Pérez-Brocal, V., and Clark, C.G. (2008). Analysis of two genomes from the mitochondrion-like
571 organelle of the intestinal parasite *Blastocystis*: complete sequences, gene content and genome
572 organization. *Mol Biol Evol* 25, 2475-2482.

573 Petersen, A.M., Stensvold, C.R., Mirsepasi, H., Engberg, J., Friis-Moller, A., Porsbo, L.J., Hammerum,
574 A.M., Nordgaard-Lassen, I., Nielsen, H.V., and Kroghfelt, K.A. (2013). Active ulcerative colitis
575 associated with low prevalence of *Blastocystis* and *Dientamoeba fragilis* infection. *Scand J*
576 *Gastroenterol* 48, 638-639.

577 Rath, A., Glibowicka, M., Nadeau, V.G., Chen, G., and Deber, C.M. (2009). Detergent binding explains
578 anomalous SDS-PAGE migration of membrane proteins. *Proceedings of the National Academy of*
579 *Sciences* 106, 1760-1765.

580 Rhoads, D.M., Umbach, A.L., Sweet, C.R., Lennon, A.M., Rauch, G.S., and Siedow, J.N. (1998).
581 Regulation of the cyanide-resistant alternative oxidase of plant mitochondria. Identification of the
582 cysteine residue involved in alpha -keto acid stimulation and intersubunit disulfide bond formation. *J*
583 *Biol Chem* 273, 30750-30756.

584 Rigottier-Gois, L. (2013). Dysbiosis in inflammatory bowel diseases: the oxygen hypothesis. *ISME J* 7,
585 1256-1261.

586 Rivera-Chávez, F., Lopez, C.A., and Bäumlner, A.J. (2017). Oxygen as a driver of gut dysbiosis. *Free*
587 *Radical Biology and Medicine* *105*, 93-101.

588 Roberts, C.W., Roberts, F., Henriquez, F.L., Akiyoshi, D., Samuel, B.U., Richards, T.A., Milhous, W.,
589 Kyle, D., McIntosh, L., Hill, G.C., *et al.* (2004). Evidence for mitochondrial-derived alternative oxidase
590 in the apicomplexan parasite *Cryptosporidium parvum*: a potential anti-microbial agent target. *Int J*
591 *Parasitol* *34*, 297-308.

592 Shiba, T., Kido, Y., Sakamoto, K., Inaoka, D.K., Tsuge, C., Tatsumi, R., Takahashi, G., Balogun, E.O.,
593 Nara, T., Aoki, T., *et al.* (2013). Structure of the trypanosome cyanide-insensitive alternative oxidase.
594 *Proc Natl Acad Sci U S A* *110*, 4580-4585.

595 Silberman, J.D., Sogin, M.L., Leipe, D.D., and Clark, C.G. (1996). Human parasite finds taxonomic
596 home. *Nature* *380*, 398.

597 Simren, M., Barbara, G., Flint, H.J., Spiegel, B.M., Spiller, R.C., Vanner, S., Verdu, E.F., Whorwell, P.J.,
598 Zoetendal, E.G., and Rome Foundation, C. (2013). Intestinal microbiota in functional bowel disorders:
599 a Rome foundation report. *Gut* *62*, 159-176.

600 Sommer, F., Anderson, J.M., Bharti, R., Raes, J., and Rosenstiel, P. (2017). The resilience of the
601 intestinal microbiota influences health and disease. *Nat Rev Microbiol* *15*, 630-638.

602 Stairs, C.W., Eme, L., Munoz-Gomez, S.A., Cohen, A., Dellaire, G., Shepherd, J.N., Fawcett, J.P., and
603 Roger, A.J. (2018). Microbial eukaryotes have adapted to hypoxia by horizontal acquisitions of a gene
604 involved in rhodoquinone biosynthesis. *Elife* *7*.

605 Standley, D.M., and van der Giezen, M. (2012). Modeling the alternative oxidase from the human
606 pathogen *Blastocystis* using automated hybrid structural template assembly. *Res Rep Biochem* *2*, 1-
607 8.

608 Stechmann, A., Hamblin, K., Pérez-Brocal, V., Gaston, D., Richmond, G.S., van der Giezen, M., Clark,
609 C.G., and Roger, A.J. (2008). Organelles in *Blastocystis* that blur the distinction between
610 mitochondria and hydrogenosomes. *Curr Biol* *18*, 580-585.

611 Stechmann, A., Tsaousis, A.D., Hamblin, K.A., van der Giezen, M., Pérez-Brocal, V., and Clark, C.G.
612 (2009). The *Blastocystis* mitochondrion-like organelles. In *Anaerobic Parasitic Protozoa: Genomics*
613 *and Molecular Biology*, C.G. Clark, R.D. Adam, and P.J. Johnson, eds. (Horizon Scientific Press Ltd),
614 pp. 205-219.

615 Stensvold, C.R., Suresh, G.K., Tan, K.S., Thompson, R.C.A., Traub, R.J., Viscogliosi, E., Yoshikawa, H.,
616 and Clark, C.G. (2007). Terminology for *Blastocystis* subtypes - a consensus. *Trends Parasitol* *23*, 93-
617 96.

618 Stensvold, C.R., and van der Giezen, M. (2018). Associations between gut microbiota and common
619 luminal intestinal parasites. *Trends Parasitol*.

620 Tielens, A.G.M., Rotte, C., van Hellemond, J.J., and Martin, W. (2002). Mitochondria as we don't
621 know them. *Trends Biochem Sci* *27*, 564-572.

622 Tsaousis, A.D., Choudens, S.O.d., Gentekaki, E., Long, S., Gaston, D., Stechmann, A., Vinella, D., Py, B.,
623 Fontecave, M., Barras, F., *et al.* (2012). Evolution of Fe/S cluster biogenesis in the anaerobic parasite
624 *Blastocystis*. *Proceedings of the National Academy of Sciences* *109*, 10426-10431.

625 Tsaousis, A.D., Gentekaki, E., Eme, L., Gaston, D., and Roger, A.J. (2014). Evolution of the cytosolic
626 iron-sulfur cluster assembly machinery in *Blastocystis* species and other microbial eukaryotes.
627 *Eukaryot Cell* *13*, 143-153.

628 van der Giezen, M. (2011). Mitochondria and the rise of eukaryotes. *BioSci* *61*, 594-601.

629 Yakoob, J., Jafri, W., Beg, M.A., Abbas, Z., Naz, S., Islam, M., and Khan, R. (2010). *Blastocystis hominis*
630 and *Dientamoeba fragilis* in patients fulfilling irritable bowel syndrome criteria. *Parasitol Res* *107*,
631 679-684.

632 Young, L., May, B., Shiba, T., Harada, S., Inaoka, D.K., Kita, K., and Moore, A.L. (2016a). Structure and
633 Mechanism of Action of the Alternative Quinol Oxidases. *Adv Photosynth Resp* *41*, 375-394.

634 Young, L., May, B., Shiba, T., Harada, S., Inaoka, D.K., Kita, K., and Moore, A.L. (2016b). Structure and
635 mechanism of action of the alternative quinol oxidases. *Adv Photosynth Resp* *41*, 375-394.

- 636 Zierdt, C.H. (1986). Cytochrome-free mitochondria of an anaerobic protozoan--*Blastocystis hominis*. J
637 Protozool 33, 67-69.
- 638 Zierdt, C.H. (1991). *Blastocystis hominis*--past and future. Clin Microbiol Rev 4, 61-79.
- 639
- 640

In review

641 **Figure legends**

642

643 **Figure 1.** Functional residues are conserved in the *Blastocystis* alternative oxidase (AOX). The
644 *Blastocystis* AOX was aligned to the *Trypanosoma brucei* and *Sauromatum guttatum* AOX
645 sequences. Residues involved in coordinating the diiron in the active site are indicated in
646 brown. Quinone binding residues are indicated by an orange background and possible
647 rhodoquinol coordinating residues are indicated by a yellow background. The *S. guttatum* T179
648 postulated in oxygen affinity has been indicated by a yellow background and an orange rim.
649 The epitope recognized by the *S. guttatum* AOX monoclonal antibody is indicated by a brown
650 box.

651

652 **Figure 2.** *Blastocystis* alternative oxidase (AOX) homology modelling from the trypanosomal
653 alternative oxidase (TAO) crystal structure (PDB:5GN2) generated using the Swiss-model
654 software (<http://swissmodel.expasy.org/>). A. Surface representation of the model, with
655 hydrophobic residues coloured orange. B. Primary and secondary ligation sphere, with
656 numbering based on the TAO amino acid numbering. Non-conserved amino acids are labelled
657 in parenthesis. C. and D. show the same docked rhodoquinol (magenta) from two different
658 orientations. Amino acids shown as sticks are all within 6 Å of the substrate, with potential
659 hydrogen bonds to (E215H) (T219S) and the iron core shown as yellow dotted lines. Atoms
660 are coloured as yellow for carbon, blue for nitrogen and red for oxygen, with the iron core as
661 orange spheres.

662

663 **Figure 3.** The *Blastocystis* alternative oxidase (AOX) is enriched in mitochondrial fractions.
664 A. Western blot analyses of the expression and cellular localisation of *Blastocystis* AOX, the
665 *Blastocystis* mitochondrial marker hydrogenase and cytosolic marker SufCB. B. Typical SDS-
666 PAGE gel of protein extracts from whole cells, mitochondrial and cytosolic fractions of
667 *Blastocystis* stained with Coomassie blue.

668

669 **Figure 4.** The *Blastocystis* alternative oxidase (AOX) is localised in the mitochondrion.
670 Several *Blastocystis* cells are shown. A. anti-AOX antibody recognizes several discrete
671 locations in *Blastocystis*. B. Staining of the mitochondrion-like organelles with MitoTracker.
672 C. DAPI staining of DNA in the mitochondria and in the nucleus. D. Overlay of anti-AOX and
673 Mitotracker demonstrating the co-localization of signal. E. Merged of all signals with co-
674 localization of anti-AOX, Mitotracker and DAPI in the mitochondria and DAPI alone for the
675 *Blastocystis* nuclei. F. DIC image of the *Blastocystis* cells. Bar is 5 µm.

676

677 **Figure 5.** Oxygen uptake by *Blastocystis* alternative oxidase (AOX) in *Escherichia coli*. A.
678 Oxygen levels were allowed to stabilise before addition of heme deficient *E.coli* membranes
679 expressing recombinant *Blastocystis* AOX. Addition of duroquinol (DQH2) (final
680 concentration of 1 mM) induced oxygen consumption. Oxygen uptake was sensitive to a typical
681 AOX inhibitor octylgallate (OG). Octylgallate was added to a final concentration of 25 µM.
682 Oxygen consumption was not due to the action of complex IV as protein was expressed in
683 heme deficient *E. coli* and functional complex IV cannot be produced by these cells.
684 Furthermore, antimycin A, a complex III inhibitor, was added (AA) to a final concentration of

685 1 μ M. Rates shown on the graph are nmols O₂ consumed/min/mg protein. B. Oxygen
686 consumption by whole *E. coli* FN102 cells expressing *Blastocystis* AOX (orange trace) was
687 measured using a high-resolution respirometer compared to *E. coli* cells not expressing the
688 *Blastocystis* AOX (brown trace). Oxygen consumption is roughly three times higher in the
689 AOX expressing strain and sensitive to the AOX inhibitor salicylhydroxamic acid (SHAM).
690 Three independent experiments were conducted and a representative data set is presented.

691

692 **Figure 6.** The *Blastocystis* alternative oxidase (AOX) is sensitive to salicylhydroxamic acid
693 and thenoyltrifluoroacetone. A. Routine respiration was determined in *Blastocystis* cells diluted
694 to a density of 1×10^6 cells/ml before the addition of the AOX inhibitor salicylhydroxamic acid
695 (SHAM) in two sequential 2.4 mM doses. Following SHAM addition the succinate
696 dehydrogenase (Complex II) inhibitor thenoyltrifluoroacetone (TTFA) was added to a final
697 concentration of 5.4 μ M. Shown are an average of four independent experiments. Error bars
698 represent standard deviation. B. Routine respiration was determined in *Blastocystis* cells
699 diluted to a density of 1×10^6 cells/ml before the addition of two doses of the Complex II
700 inhibitor TTFA was added to a final concentration of 5.4 μ M and 11 μ M. Following this the
701 AOX inhibitor SHAM was added in two doses to a final concentration of 2.4 mM and 4.8 mM.
702 Shown are an average of two independent experiments. Error bars represent standard deviation.

In review

Figure 1.TIF

In review

```

Blastocystis 1 -----MFPILSRVFFKREAVVFRGFSVSSYEQFIDKECISKALNKKPNEHYHIFSTRYHSSNREYLT----- 61
T. brucei 1 MFRN-----HASRITAAAAPWVLR TACRQKSDAKTPVWGHTQLNRLS FLETVPVPLRVSD ESED RP----- 62
S. guttatum 1 MMSSRLVGTALCRQLSHVPPVQYLPALRPTADTASSLLHGCSAAAPAQRAGLWPPSWFSPPRHASTLSAPAQDGGKEKAAGTAGKVPPGE 90

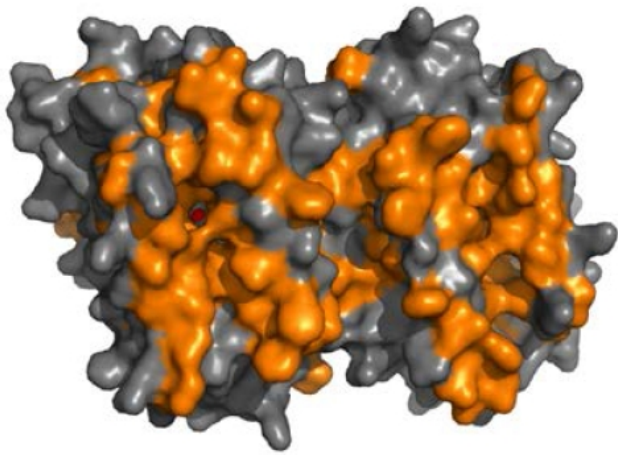
Blastocystis 62 ----- ILESCWGEQPKRH PKGVSDRVASGIVNALFKIGNAYFRENY----- IL 105
T. brucei 63 ----- TWSLP----- DIENVAITHKKPNGLVDTLAYRSVRTCRWLFDTFSLYRFGSITESKVIS 117
S. guttatum 91 DGGAEKEAVVSYWAVPPSKVSKEDGSEWRWTCFRPWETYQADLSIDLHKHHVPTTILDKLALRTVKALRWPTDIFFQRRY-----AC 172

Blastocystis 106 RAVFLESVASIPGLVCSNLHHLRCLRRLQPD-SWIKPLVDEAENERMHLLAVR TYTKLTAVQKLFIRITQFSFVTLFSFLVFAPRTSHR 194
T. brucei 118 RCLFLETVAGVPGMVGMLRHLSSLRYMTRDKGWINTLLVEAENERMHLMTFIELRQGPLLRVSIITQAIMYLFLLVAYVISPRFVHR 207
S. guttatum 173 RAMMLETVAAVPGMVGGLLHLKSLRRFEHSGGWIRALLEEAENERMHLMTFMEVAQPRWYERALVLAVQGVFFNAYFLGYLLSPKFAHR 262

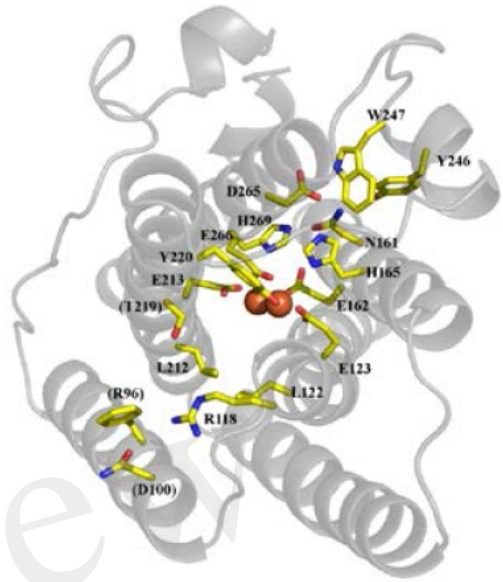
Blastocystis 195 LVGFLEEHAVDSYTEMIRRIDSN TLENRP--ATQITKDYWGLPEDATLRDALLVIRADEADHRLVNHSLGDAYDKKTPVSVKKWYAGCAF 282
T. brucei 208 FVGYLEEEAVITYTGVMRAIDEGRLRPTKNDVPEVARVYWNLSKNATFRDLINVIRADEAEHRVNHHTFADMHEKRLQNSVNPFFVLLKKN 297
S. guttatum 263 VVGYLEEEA IHSYTEFLKDIDSGAIQDCP--APAIALDYWRLPQGSTLRDVVTVVIRADEAHRDVNH FASDVHYQDLELKTTPAPLGYH- 349

Blastocystis 283 PVNLHEPFGPYMDFSKYGATKA-----
T. brucei 298 PEEMYSNQPSGKTRTDFGSEGAKTASNVNKHV
S. guttatum -----
    
```

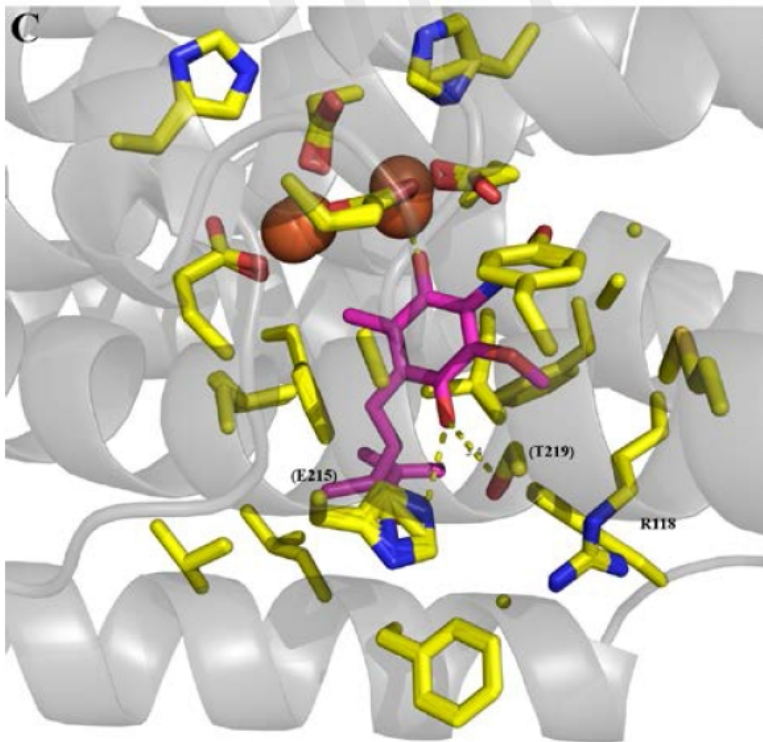
A



B



C



D

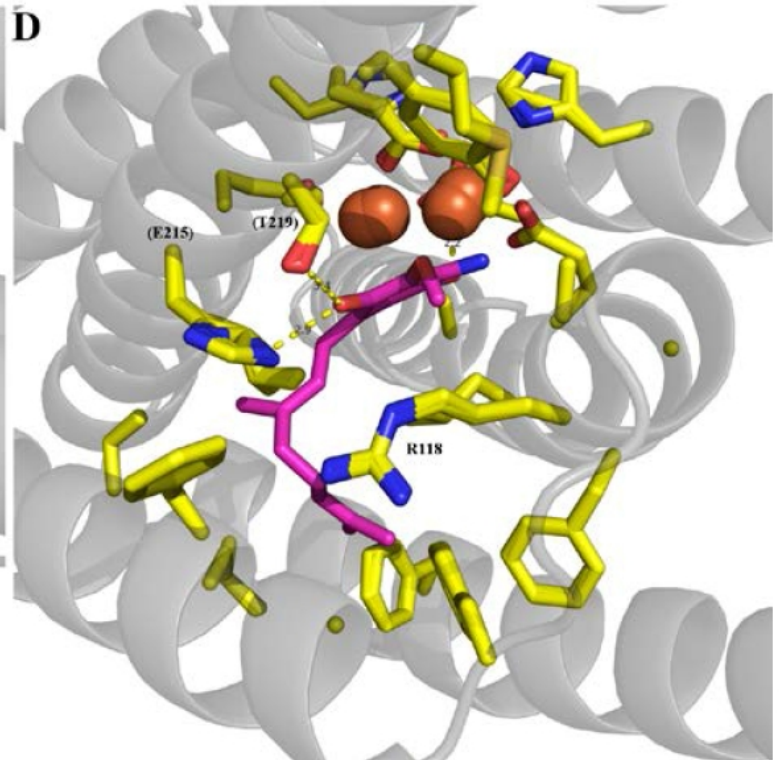


Figure 3.TIF

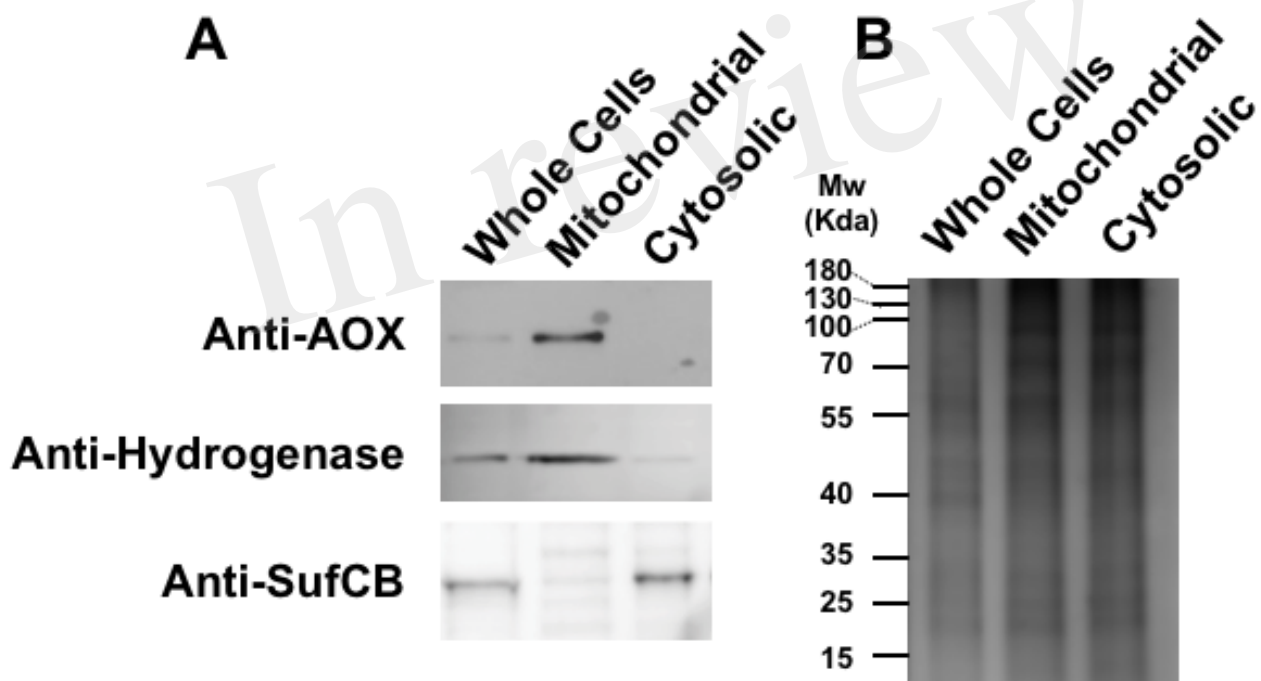


Figure 4.TIF

In review

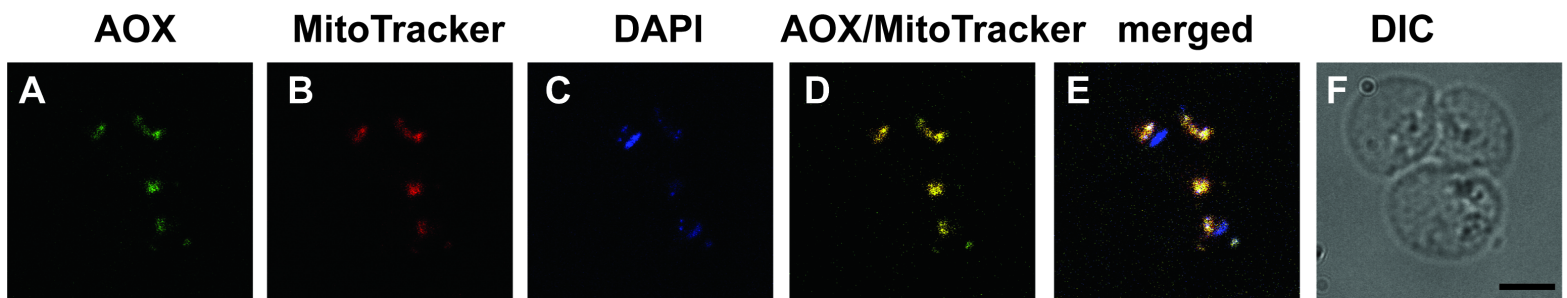


Figure 5.JPEG

In review

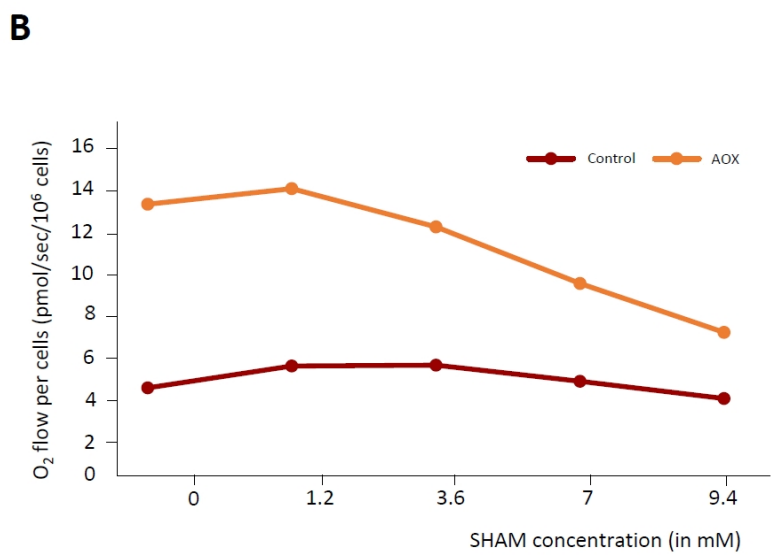
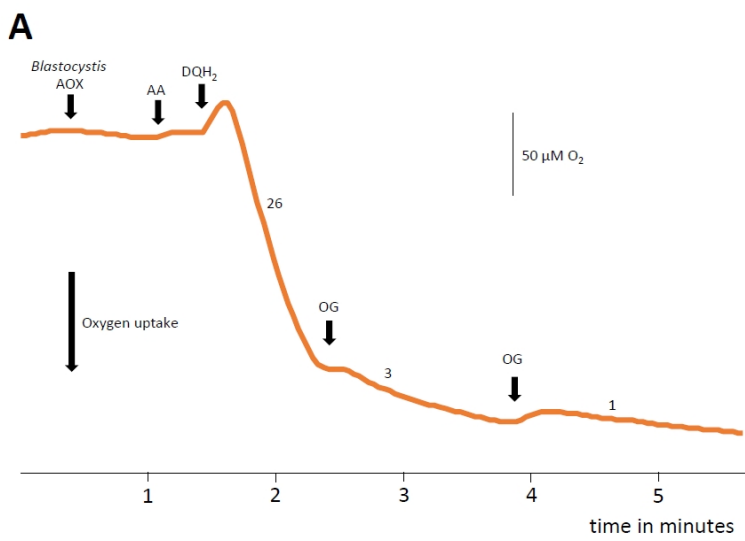


Figure 6.TIF

